

Study of Etching Pits in a Large-Grain Single Cell Bulk Nb Cavity*

X. Zhao[#], G. Ciovati, C. E. Reece, and A. T. Wu
Jefferson Lab, Newport News, VA 23606, U.S.A.

ABSTRACT

Performance of SRF cavities are limited by non-linear localized effects. The variation of local material characters between "hot" and "cold" spots is thus of intense interest. Such locations were identified in a BCP-etched large-grain single-cell cavity and removed for examination by high resolution electron microscopy (SEM), electron-back scattering diffraction microscopy (EBSD), optical microscopy, and 3D profilometry. Pits with clearly discernable crystal facets were observed in both "hotspot" and "coldspot" specimens. The pits were found in-grain, at bi-crystal boundaries, and on tri-crystal junctions. They are interpreted as etch pits induced by surface crystal defects (e.g. dislocations). All "coldspots" examined had qualitatively low density of etching pits or very shallow tri-crystal boundary junction. EBSD revealed the crystal structure surrounding the pits via crystal phase orientation mapping, while 3D profilometry gave information on the depth and size of the pits. In addition, a survey of the samples by energy dispersive X-ray analysis (EDX) did not show any significant contamination of the samples surface.

MOTIVATION

- Some SRF accelerator cavities made of high-purity bulk Nb (RRR~300) prepared by BCP suffer "Q-drop" at field gradients above ~20 MV/m or ~100 mT. The causes of this phenomenon have not yet been fully elucidated.
- In addition, anomalous rf losses have been observed in the medium field range ($E_{acc} \sim 5\text{-}20$ MV/m). Understanding this is important for the development of CW superconducting accelerators.
- To study this topic, a surface analysis study was undertaken on samples cut from a single cell cavity made of large-grain Nb which exhibited a strong medium field Q-slope.
- Samples were cut from locations where anomalous heating was detected by thermometry ("hotspots") as well as from locations with negligible overheating ("coldspots").

PREPARATION OF SRF CAVITY

The investigated single cell 1.5 GHz SRF cavity is made from large grain plates cut from ingot B produced by Companhia Brasileira de Metalurgia e Mineração (CBMM, Sao Paulo, Brasil). Ingot B had several large grains in-plane. RRR value of the material was ~280 with a Ta content of ~800 ppm. The cavity had experienced the following processes:

- Large grain sheets sliced from ingot "B" (CBMM) by wire-EDM
- A deep-drawing process deforming the plates to half cells.
- Prior to the equator weld, ~10 min etching by **Buffered Chemical Polishing** (BCP) with HNO_3 , HF, H_2PO_4 1:1:1 by volume
- Electron beam weld was done inside and outside.
- After welding, the weld was mechanically ground.
- The beam tubes were welded in the end to the irises.
- The cavity was heat treated at 600°C/10h, then etched ~10+60 μm by BCP 1:1:1 before first rf test.

PERFORMANCE OF THE SRF CAVITY

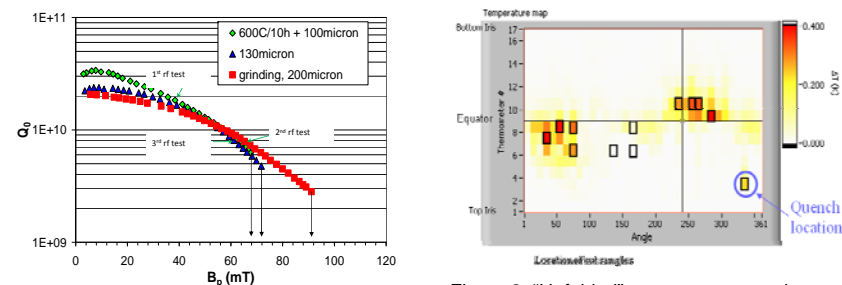
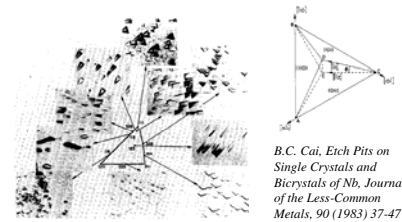


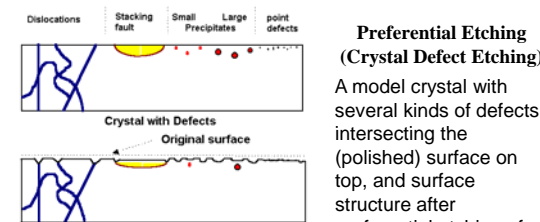
Figure 1: Q_0 vs. B_p at 1.7 K

- The results of the first rf test at 1.7 K are shown in Figure 1. The quality factor, Q_0 , monotonically decreased for increasing peak surface magnetic field, B_p , up to 68 mT, where quench occurs.
- The cavity performance did not improve significantly after an additional 30 μm etching by BCP 1:1:1. Temperature mapping showed the quench location to be on the cell's side wall, closer to the iris.
- A large defect ("hole") was visible by naked eye in that area. Repair of the defect was attempted by mechanical grinding, followed by an additional ~70 μm removal by BCP 1:1:1.
- The following rf test showed an improvement of the quench field, occurring at the same location as before. The Q_0 vs. B_p curve was still characterized by a strong medium field Q-slope. No field emission was detected during any of the RF tests.
- Several "hotspot" are visible in the equator area. The location of the hotspots did not change significantly with successive material removal by BCP.

ETCHING PITS ARE WELL KNOWN FOR CRYSTAL ETCHING



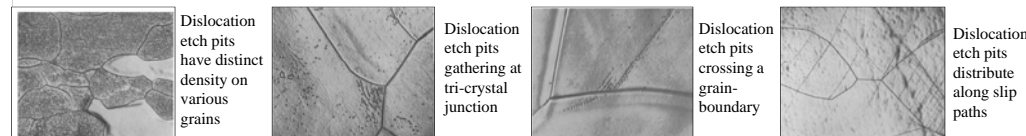
Schematic of a 3-d etching pit. The tetrahedral pit is composed of three {110} planes with a {111} plane as the etching surface



Dislocations, Stacking fault, Small Precipitates, Large point defects. Preferential Etching (Crystal Defect Etching). A model crystal with several kinds of defects intersecting the (polished) surface on top, and surface structure after preferential etching of defects.

Dislocation => Etching Pits
Grain Boundary => Etching Groove and Steps

Excerpt from http://www.ifam.fz-juelich.de/marcus/amats/def_en/sap_6/backbone/r6_1_1.html#_4



P.R. Evans, Dislocation Etch Pit Studies in Annealed and Deformed Polycrystalline Nb, Journal of Less Common Metals, 6 (1964) 253-265

FEATURE OF ETCHING PITS ON THE CAVITY SURFACE

Sampl e No.	No. of grains	Location	Pits Density (# per mm ²)	Feature
1	2	Hotspot	34.2	
2	1	Hotspot	29.1	Quench site
3	3	Hotspot		
4	3	Hotspot		
5	3	Hotspot	61.7	a very deep pit on tri-crystal junction; on {110} plane, hidden elongated etching pits
6	1	Coldspot	6.3	
7	3	Coldspot	19.7	a shallow pit on tri-crystal junction
8	1	Coldspot	17.6	
9	3	Hotspot		a very deep pit on tri-crystal junction
10	1	Hotspot		
11	1	Hotspot		
12	2	Hotspot		

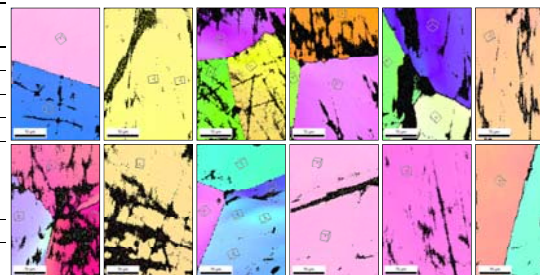


Figure 3: Grain orientation of the 12 samples. Samples 1-6 are at the first row (L to R). Samples 7-12 are at the second row (L-R). Their orientation are presented by Inversed Pole Figure (IPF) color map. The triangle IPF color legend (Nb [100]) is on left.

Table 1: Features observed on the 12 samples dissected from the large-grain single cell cavity.

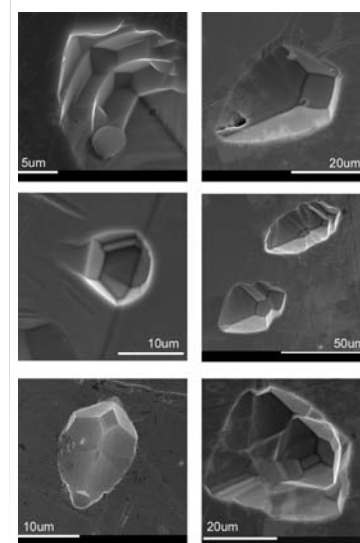


Figure 4: Etching pits with complex and symmetric geometry are observed in contrast to typical tetrahedral pits. Their formation mechanism is under investigation.

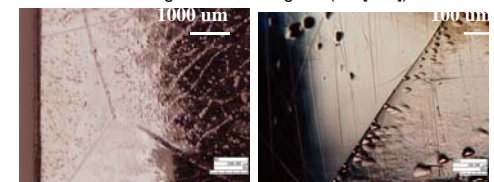


Figure 5: Optical imaging of Sample 9, showing pit density varies on distinct crystal grains.

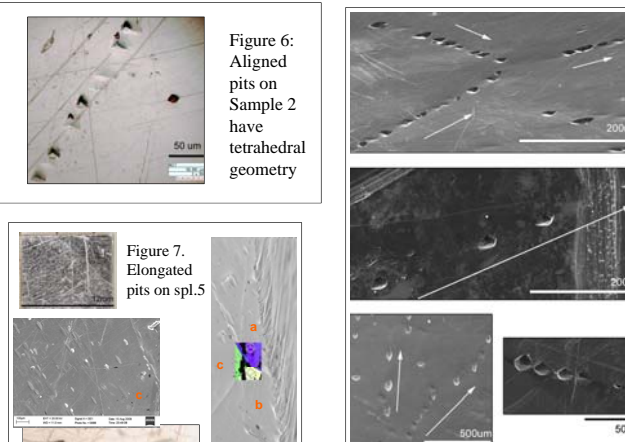


Figure 6: Aligned pits on Sample 2 have tetrahedral geometry

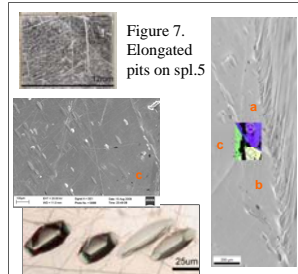


Figure 7: Elongated pits on spl.5

Figure 8: Pits might distribute on a dislocation slip path

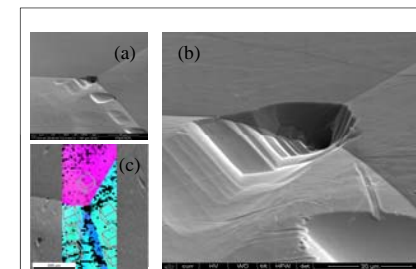


Figure 9. a-b) Etching pit at a tri-crystal junction (Sample 9); c) Crystal orientation map via EBSD revealing the three crystal orientations

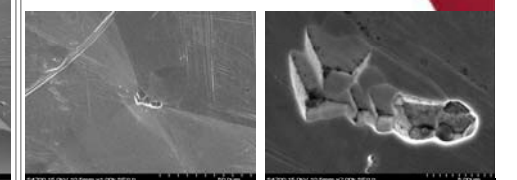


Figure 10. Etching pit of Sample 7 on tri-crystal junction

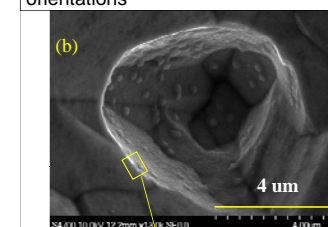


Figure 11. a-b) from sample 5 (Left). Etching pit at the tri-crystal junctions have deep, sharp profiles. The pit diameter is ~5 μm and its **curvature radius ~50 nm**. Thus, its aspect ratio is ~100.

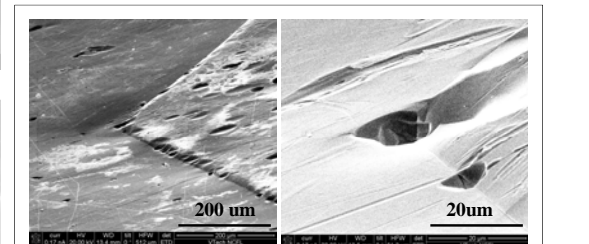
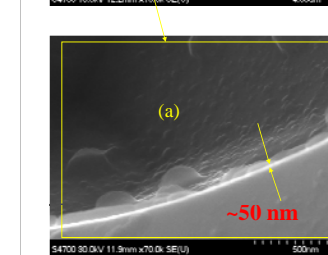


Figure 12. Etching pits on a bicrystal junction (Sample 3)

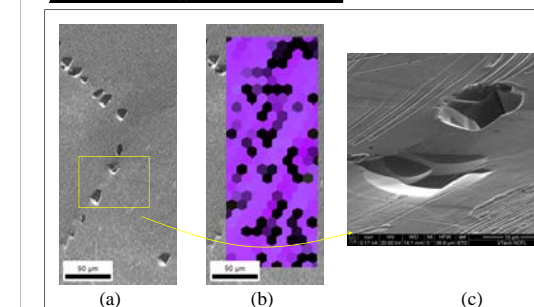


Figure 13. Etching pits on the single crystal grain of Sample 3. a) & c) SEM micrograph b) Inverse pole figure (IPF via EBSD) indicates the crystal orientation is [111].

DISCUSSION AND SUMMARY

- By experiments [6] and simulations [2], one expects that magnetic field enhancement at sharp edges, such as grain boundaries, pits or other defects, may cause local and/or global quench.
- RF and temperature measurements of this cavity indicate monotonic losses, already starting at very low field ($B_p \sim 20$ mT). The hypothesis of local quenches starting at such low field would imply enhancement factors of about 10. (Which per [2] would require aspect ratios of 1000 with local radius of curvature 50 nm.)
- Features of this high aspect ratio (1000) have not been observed yet via SEM.
- Etching pits observed in this study are uncommon to the surface of large-grain BCP-etched cavities, and the cause for their nucleation on this particular cavity is still unclear.

ACKNOWLEDGMENTS

We thank G. Slack for the careful cavity dissection. We acknowledge Dr. M.Y. Zhu and the College of William & Mary for their support on SEM measurements. We appreciate Olga Trofimova carefully counting the pit density. We thank Prof. Bieler (Michigan State University) for fruitful conversations regarding dislocation-induced etching pits.

REFERENCES

- P. Kneisel, G.R. Myneni, G. Ciovati, J. Sekutowicz, T. Carneiro, "Development of Large Grain/Single Crystal Niobium Cavity Technology at Jefferson Lab", Single Crystal Niobium Technology Workshop, CBMM, Araxa, Brazil, Nov. 2006
- V. Shemelín, H. Padamsee, TTC-Report 2008-07, SRF 080903-04, TESLA 2008
- H. Padamsee, SO Meeting, Jan 26, 2009
- B.C. Cai, A. Dasgupta and Y.T. Chou, Journal of the Less-Common Metals, 90(1983):37-47
- P.R. Evans, Journal of the Less-Common Metals, 6(1964) 253-265
- S. Berry, C. Antoine and M. Desmons, "Surface Morphology at the Quench Site", EPAC'04, Lucerne, July 2004, TUPKF018, p. 1000 (2004).
- Etching of Crystals, Theory, Exp., and Apl., Sangwal, ISBN 0 444 87018 0